# Polybenzimidazole Membranes for Hydrogen and Sulfuric Acid Production in the Hybrid Sulfur Electrolyzer

Jai Vishnuvarman Jayakumar, Alexander Gulledge, John A. Staser, Chang-Hee Kim, Brian C. Benicewicz and John W. Weidner

| Email alerting service | Receive free email alerts when new articles cite this article - sign up in the box at the top right corner of the article or  click here |
| --- | --- |

# Polybenzimidazole Membranes for Hydrogen and Sulfuric Acid Production in the Hybrid Sulfur Electrolyzer

**Jai Vishnuvarman Jayakumar,**[a,*] **Alexander Gulledge,**[b] **John A. Staser,**[a,**] **Chang-Hee Kim,**[c] **Brian C. Benicewicz,**[b] **and John W. Weidner**[a,***,z]

[a]*Center for Electrochemical Engineering, Department of Chemical Engineering, University of South Carolina, Columbia, South Carolina 29208, USA*
[b]*Department of Chemistry, University of South Carolina, Columbia, South Carolina 29208, USA*
[c]*Hydrogen and Fuel Cell Department, Korea Institute of Energy Research (KIER), Yuseong-gu, Daejeon 305-343, Korea*

The hybrid sulfur (HyS) thermochemical cycle has been investigated as a means to produce large quantities of clean hydrogen at efficiencies higher than those possible from water electrolysis. Recent studies have shown that traditional proton exchange membranes, such as Nafion, may limit HyS electrolyzer performance because concentrated sulfuric acid produced during electrolysis dehydrates the membrane. In this paper, we report the use of sulfonated polybenzimidazole (s-PBI) membranes in the HyS electrolyzer. The advantage of s-PBI membranes over Nafion is that conductivity does not decrease at low water content. We have evaluated s-PBI membranes over a range of current densities at 80 and 90°C, and report favorable performance compared to that of Nafion with the possibility of producing higher sulfuric acid concentrations and lower voltages at elevated temperatures.
© 2012 The Electrochemical Society. [DOI: 10.1149/2.010206eel] All rights reserved.

The hybrid sulfur (HyS) thermochemical cycle has garnered considerable attention lately because of its potential to produce clean hydrogen on a large scale at efficiencies higher than those possible for water electrolysis.[1–20] The two-step HyS process relies on the high-temperature (~900°C) decomposition of $H_2SO_4$ to $SO_2$, $O_2$ and $H_2O$, and the low-temperature (~100°C) electrochemical oxidation of $SO_2$ in the presence of water to produce $H_2SO_4$ and $H_2$. Since the sulfur compounds are internally recycled, the overall process is the decomposition of water to $H_2$ and $O_2$. The process is interesting because the high-temperature decomposition step could be coupled to next-generation nuclear power plants or high-temperature solar arrays.[1–7] In the electrolysis step, $SO_2$ is oxidized at the anode via the following reaction:[11,14–19]

$$SO_2 + 2H_2O \rightarrow H_2SO_4 + 2H^+ + 2e^- \quad U^0_{SO_2} = 0.158 \text{ V vs. SHE}$$
[1]
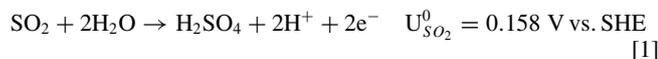
The protons produced in Reaction 1 migrate through the membrane and reduce to hydrogen at the cathode:

$$2H^+ + 2e^- \rightarrow H_2 \quad U^0_{H_2} = 0 \text{ V vs. SHE}$$
[2]
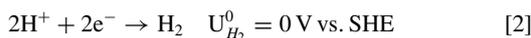
Reactions 1 and 2 have been successfully conducted over a range of operating conditions (e.g., temperature, $SO_2$ flow rate, membrane pressure difference) and design variations (e.g., catalyst loading, membrane type and thickness).[14–17] For a gas-fed anode using a proton-exchange membrane (PEM) such as Nafion in the electrolyzer, we have accurately predicted water transport and used that to calculate cell voltages and sulfuric-acid concentrations as a function of operating and design variables.[15–19] One insight from this work[19] is that the concentration of sulfuric acid increases with current density, which dehydrates the membrane and increases its resistance.[19,21,22] This creates a challenge when using a PEM electrolyzer in the HyS process. That is, the production of concentrated sulfuric acid is desired to improve the efficiency of the high-temperature decomposition step, but undesired because it dehydrates the membrane and reduces the efficiency of the electrolysis step of the cycle.[19]

Acid-doped polybenzimidazole (PBI) membranes represent an alternative to Nafion because they do not rely on water for their proton conductivity, and therefore they offer the possibility of operating at high acid concentrations and/or elevated temperatures to minimize voltage losses (e.g., kinetic and ohmic resistances). Early studies relied on doping the already-cast PBI membranes with concentrated solutions of phosphoric acid (up to 11 *M*) to impart conductivity to the membrane.[23,24] The phosphoric acid-doped PBI membranes exhibited good conductivity at temperatures above 100°C, low gas permeability and low electro-osmotic drag.[24] While the approach yielded sufficiently conductive PBI membranes for high temperature fuel cell operation, leaching of the phosphoric acid over time resulted in a gradual loss of conductivity.

More recently, an alternative casting and doping procedure was developed for a variety of PBI membranes, termed the PPA process.[25,26] This process relies on polyphosphoric acid (PPA) as the polycondensation agent, the polymerization solvent, and the casting solvent. The polymerized PBIs are cast directly from the PPA solution and membrane formation occurs when moisture is absorbed from the atmosphere, which hydrolyzes the PPA to phosphoric acid in the membrane. Sulfonated PBI (s-PBI) membranes can be prepared using the same process starting with sulfonated monomers to impart an additional acid moiety in the polymer structure to enhance conductivity.[27] Here we report the use of s-PBI membranes in the HyS electrolyzer and compared it to data collected from a Nafion-based cell.

## Experimental

Sulfonated PBI (s-PBI) membranes (thickness controlled to 500 μm) were prepared as described earlier.[27] The only difference between the already-reported s-PBI membranes and those used in this study is an additional acid exchange step. After casting from PPA and hydrolysis to phosphoric acid, the s-PBI membranes were soaked in deionized water at room temperature for 5 days to remove the phosphoric acid. The leached s-PBI membranes were then immersed in 5 *M* sulfuric acid for 2 days prior to use. Titrations were conducted using a Metrohm 716 DMS Titrino automated titrater and a standardized 0.1 *M* sodium hydroxide solution. The acid exchange was confirmed using the difference in pKa and equivalence points between sulfuric acid (−3, 1.92) and phosphoric acid (2.15, 7.20, 12.35) respectively. Moreover, titration across the full spectrum revealed only two equivalence points, verifying that only sulfuric acid remained in the membrane. In addition to verification of acid exchange, titration experiments were conducted as previously reported to obtain membrane composition (i.e. acid doping level and polymer content).[28] Experimental studies reported were conducted with membranes containing doping levels of 17.8 mol $H_2SO_4$ per mol PBI.

Membrane electrode assemblies (MEAs) were constructed by hot-pressing gas diffusion electrodes (1.0 mg Pt/cm²) obtained from BASF to each side of the s-PBI membranes as described previously.[29] The MEAs made with Nafion 117 (175 μm thick) and 212 (50 μm thick)
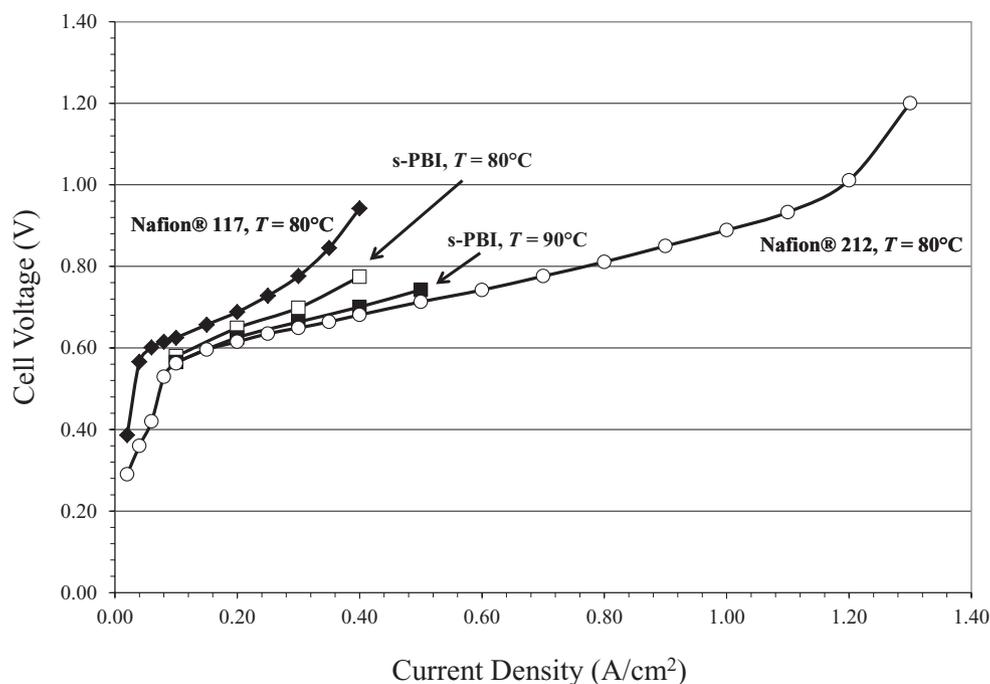
**Figure 1.** Current-voltage (*i-V*) curves from a HyS elecrolyzer using Nafion 117 (♦) and 212 (○) membranes at 80°C, with a liquid cathode and dry anode. Also shown are *i-V* curves for the electrolyzer using s-PBI membrane at 80 (□) and 90°C (■), with a dry cathode and humidified anode. The lines connect the symbols.

membranes were loaded with 1.5 mg Pt/cm$^2$ on each side using a procedure described previously.[14,15] The MEAs were loaded into a single cell purchased from Fuel Cell Technologies, Inc. The cell was 10 cm$^2$, and consisted of graphite blocks with flow channels machined into them sandwiched between two aluminum endplates to provide compression. Teflon tubing was passed through the face of the aluminum endplates directly into the graphite blocks for the reactants (i.e., SO$_2$ and water vapor) and products (sulfuric acid and water vapor). In this experimental setup, contact between the aluminum endplates and sulfuric acid was prevented. The cell was heated by heating rods inserted into the aluminum endplates. Gaseous SO$_2$ was fed into the anode compartment via a mass-flow controller at a rate corresponding to 5% conversion at each current. That is, 20 times as much SO$_2$ was fed than the stoichiometric amount required. We previously reported that the percent conversion of SO$_2$ (i.e., SO$_2$ flow rate) had little effect on performance.[14] The conversion of SO$_2$ was kept low to ensure a sufficient amount of water entered the cell, as described below.

The difference between the setups for evaluating either the s-PBI or the Nafion membranes centers on the humidification of the gaseous SO$_2$. When using Nafion-based MEAs, dry SO$_2$ gas was fed to the anode and liquid water to the cathode. The water needed to sustain Reaction 1 diffuses across the membrane due to a water activity gradient and a pressure difference. When using an s-PBI-based MEA, liquid water in contact with this membrane could accelerate leaching of the acid and lead to a gradual reduction in conductivity. Therefore, for these experiments the cathode was kept dry and the gaseous SO$_2$ was humidified prior to introduction to the anode. The humidifier was maintained at the same temperature as the electrolyzer, which was 80 and 90°C. Prior to applying the current, the water content of the SO$_2$ stream was measured by condensing out the water at the exit to the cell. For all SO$_2$ flow rates, the mole fraction of water was approximately 30 and 41 mole% at 80 and 90°C, respectively, which corresponds to 60% relative humidity at both temperatures. The resulting fractional conversion of water at all currents was 25 and 15% at 80 and 90°C, respectively.

During cell operation, the sulfuric acid was collected at the exit of the cell and titrated against sodium hydroxide to determine the concentration. Membrane resistance was measured during operation by a high-frequency milliohm meter in the current interrupt technique, in which the applied current was abruptly changed and the transient potential response was monitored.

## Results and Discussion

Figure 1 shows the current-voltage (*i-V*) curves for s-PBI at 80 and 90°C operated with a dry cathode, humidified SO$_2$ anode and no membrane pressure difference (i.e., $\Delta P = 0$). Also shown for comparison are *i-V* curves for N117 and N212 at 80°C, operating with a wet cathode and dry anode, and a membrane pressure difference of $\Delta P = 600$ kPa. From the *i-V* curves, the s-PBI operates at lower cell voltages than N117 over the full range of current densities even though the former is almost 3 times thicker. For example, at 0.3 A/cm$^2$, the cell voltage of the N117 electrolyzer is 0.776 V, while for s-PBI at the same temperature (80°C) and current density, the voltage is 0.698 V, an improvement of 0.078 V. At 90°C, where electrode kinetics should be improved, the s-PBI cell voltage at 0.3 A/cm$^2$ is 0.664 V, an improvement of 0.034 V over the 80°C operation. The N212 electrolyzer operated at a lower voltage (i.e., at 0.3 A/cm$^2$, N212 is 0.649 V vs. 0.698 V for s-PBI). The s-PBI performance improves at 90°C so that it has a similar voltage to the N212 performance at 80°C up to 0.5 A/cm$^2$. Above this current density (and above 0.4 A/cm$^2$ at 80°C), we were unable to record stable cell voltages. This may be due to excess liquid in the cell, which we plan to rectify by operating at higher temperatures.

Figure 2 shows the concentration of sulfuric acid produced during cell operation, corresponding to the *i-V* curves in Fig. 1. The Nafion 117 MEAs produces the most concentrated sulfuric acid over all current density ranges, followed by Nafion 212 and s-PBI MEAs. One dashed line is drawn through the s-PBI data at both temperatures because there is no significant difference between these data sets. There is also more scatter in these data due to slight fluctuations in the temperature of the humidifier, which can significantly affect the anode water content at these temperatures. As shown previously for the Nafion-based MEAs,[15] thinner membranes lead to greater water transport across the membrane and lower sulfuric acid concentration. The water content in the anode for the s-PBI system, on the other hand, does not rely on the transport of water through the membrane.
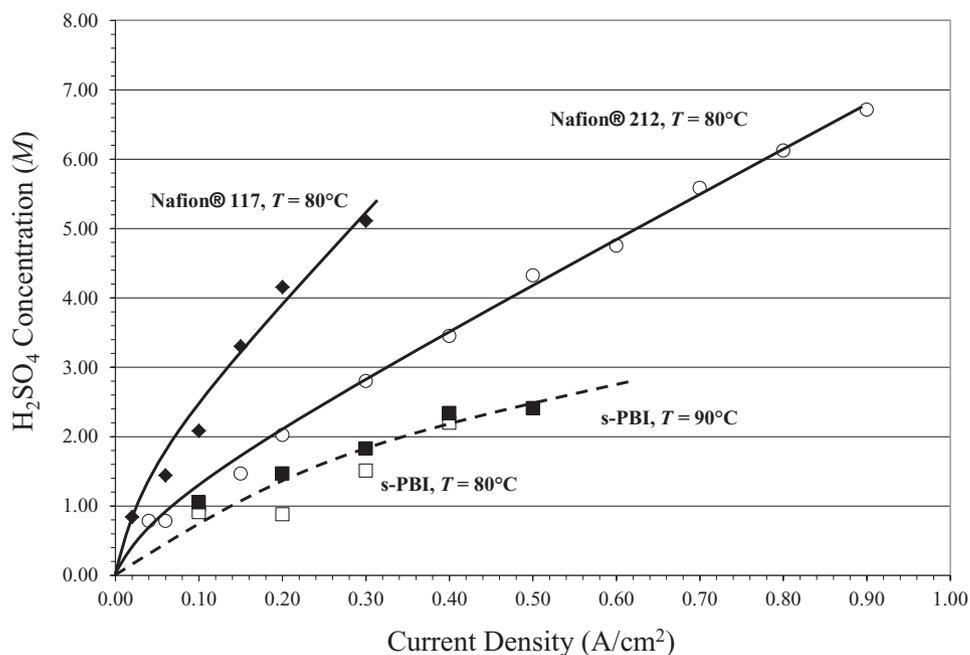
**Figure 2.** Sulfuric acid concentrations for N117 (♦) and N212 (○) at 80°C, and s-PBI at 80°C (□) and 90°C (■), corresponding to the *i-V* curves shown in Fig. 1. The dashed line goes through both sets of data for the s-PBI membrane, and all the lines are meant as a guide for the eye.

Rather, water is supplied by humidifying the inlet $SO_2$ stream. With nearly twice as much water fed to the anode at 90°C compared 80°C, it was expected that a higher humidification temperature would result in less concentrated sulfuric acid. The difference measured, however, is negligible.

Although the higher inlet water flow rate at 90°C did not result in more dilute sulfuric acid, it did result in more sulfuric acid production (i.e., more water) collected in the outlet stream, as shown in Fig. 3. That is, the rate at which sulfuric acid (i.e., $H_2SO_4 + H_2O$) leaves the electrolyzer is higher for runs using the s-PBI membrane at 90°C compared to 80°C, and both of these are higher than for runs using N212 or N117. We showed previously that when using Nafion, the production rate of $H_2SO_4$ (i.e., the product of the sulfuric acid flow rate and concentration) follows Faraday's law within experimental error.[15] However, the production rate of $H_2SO_4$ when using s-PBI is

25% lower than predicted by Faraday's law at 80°C and 0.4 A/cm², but 25% higher at 90°C and 0.5 A/cm². This suggests that $H_2SO_4$ is exchanging (either absorbing or leaching) with the s-PBI under these conditions. Stabilizing the s-PBI membranes under these operating conditions is the focus of future work.

Figure 4 shows previous data for the area-specific resistance (ASR) for N212 at 80°C as a function of the sulfuric acid concentration produced at the anode.[19] The broken lines for N117 and N212 are the model predictions for ASR given previously.[19] Also shown is the ASR for s-PBI at 80°C measured here. From Figure 4, it is clear that the ASR of s-PBI is higher than that of N212 (i.e., 0.105 Ω-cm² at about 2.0 *M* sulfuric acid versus 0.04 Ω-cm²), but is lower than N117 (i.e., 0.14 Ω-cm²); despite the relative thickness of s-PBI membranes (about 500 μm thick, versus 175 and 50 μm for N117 and N212, respectively). In addition, our data show that the ASR
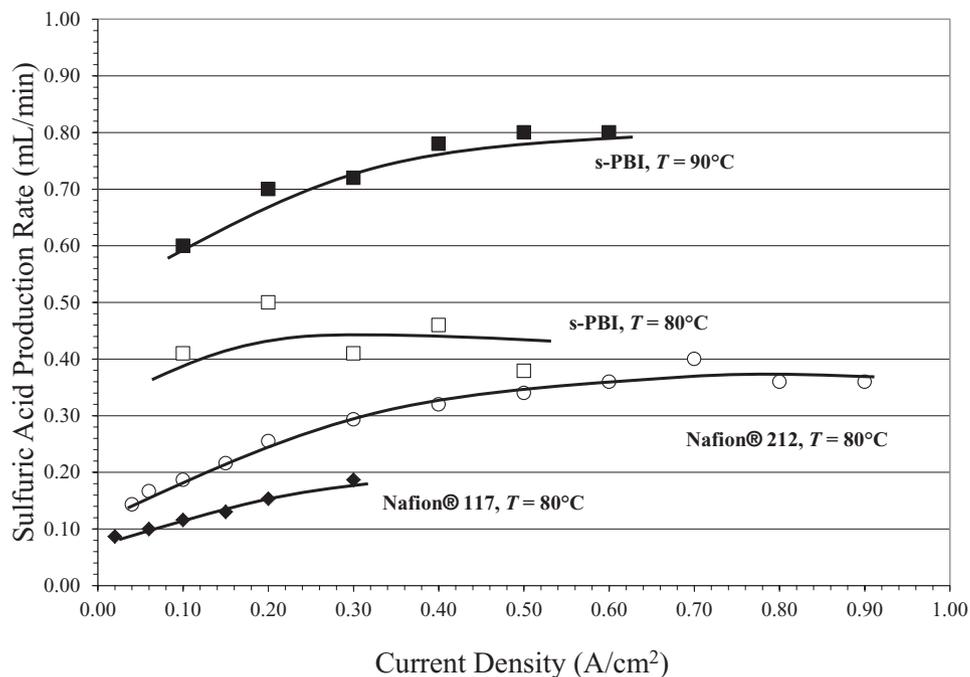


**Figure 3.** Sulfuric acid production rates for N117 (♦) and N212 (○) at 80°C, and s-PBI at 80°C (□) and 90°C (■), corresponding to the *i-V* curves shown in Fig. 1. The lines are meant as a guide for the eye.
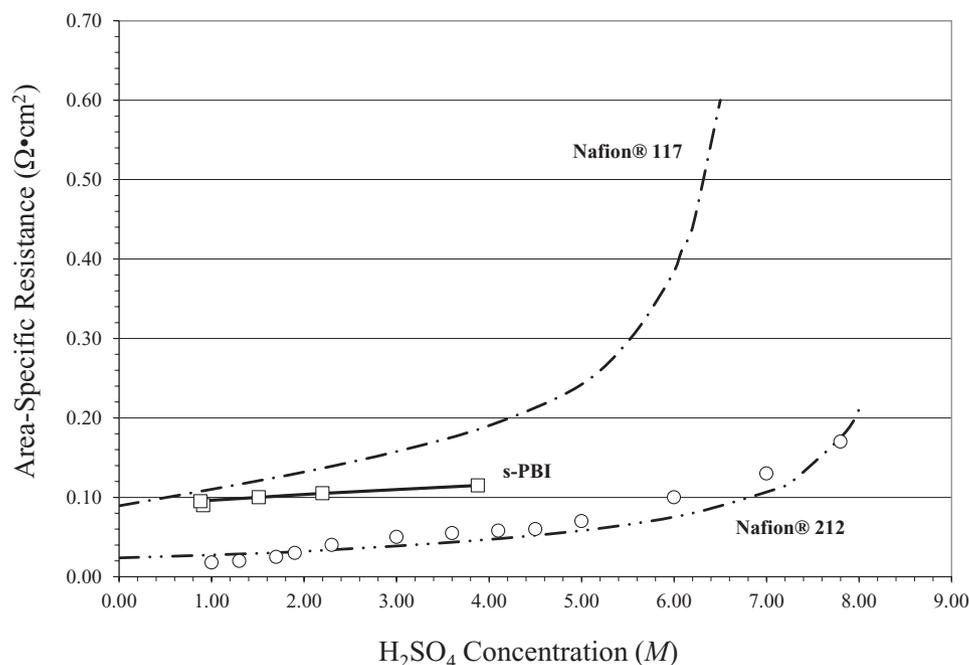
**Figure 4.** Area-specific resistance (ASR) for N212 (○) and s-PBI all at 80°C (□) as a function of sulfuric acid concentration produced at the anode. Lines for N117 and N212 are model predictions[19] and the one for s-PBI is connecting the symbols.

of s-PBI is relatively constant with increasing sulfuric acid concentrations. In contrast, the Nafion membranes exhibit an exponentially increasing ASR at high acid concentrations due to membrane dehydration. For example, with 1 $M$ sulfuric acid at the anode, the ASR of N212 is 0.018 $\Omega$-cm$^2$, for N117 it is 0.105 $\Omega$-cm$^2$, and for s-PBI it is 0.09 $\Omega$-cm$^2$. At a sulfuric acid concentration of 3.9 $M$, the ASR of N212 is 0.056 $\Omega$-cm$^2$ (an increase of 311%), for N117 it is 0.185 $\Omega$-cm$^2$ (an increase of 76%) and for s-PBI it is 0.115 $\Omega$-cm$^2$ (an increase of 28%). The rate of increase in ASR for Nafion is substantially greater beyond 4 M.

The ability of s-PBI membranes to tolerate high acid concentrations is consistent with previous data reported for s-PBI membranes immersed in greater than 7 $M$ sulfuric acid, which exhibited a lower ASR than Nafion membranes.[27] Although the experimental conditions

for those measurements are different than the ASR obtained from current interrupt measurements on an operating cell reported here, it does support our assumption that s-PBI membranes will not be adversely affected by high acid concentration, unlike Nafion. Further, because ASR is a function of membrane thickness (unlike intrinsic resistivity), it is reasonable to expect that thinner s-PBI membranes may exhibit even lower ASR.

Knowing the ASR of the various membranes, we can correct the cell voltages shown in Fig. 1. These *iR*-corrected cell voltages are shown in Fig. 5 for the data collected at 80°C. The symbols are the experimental data, and the lines for N212 and N117 are best-fit logarithmic functions through the data. The line for the s-PBI membrane is a connection of the experimental data points meant to guide the eye. The *iR*-corrected data removes the effect of an
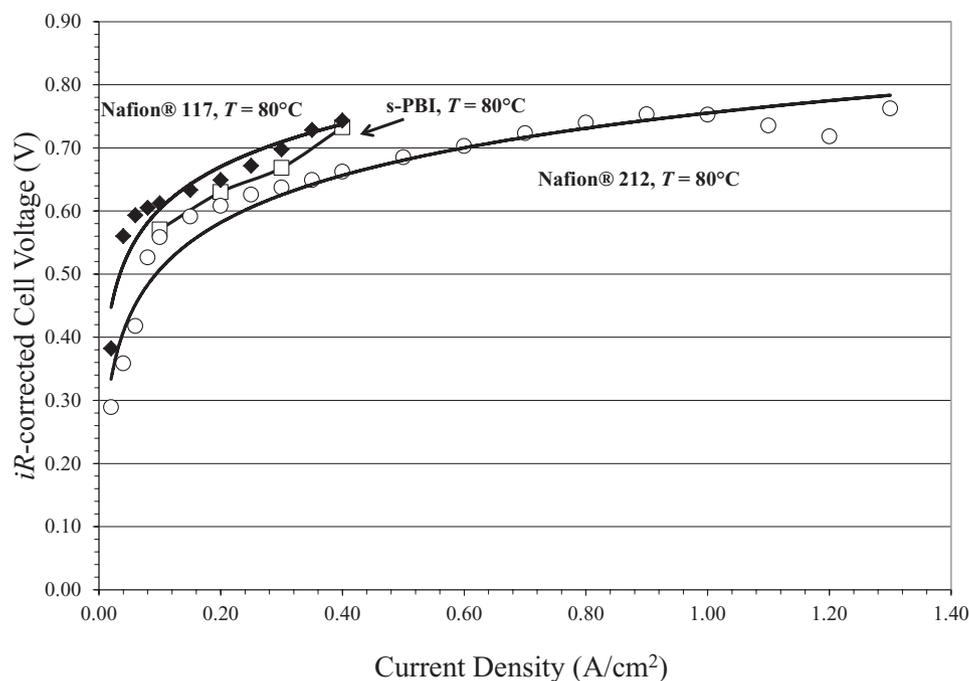


**Figure 5.** *iR*-corrected cell voltages from Fig. 1 for N117 (♦), N212 (○) and s-PBI (□) at 80°C. The lines through the N117 and N212 data are best-fit logarithmic functions through the data and the one for s-PBI is connecting the symbols.

increasing omhic resistance with increasing current for Nafion seen in Fig. 4. This highlights the fact that the remaining resistance in the HyS electrolzyer is anode kinetics, as shown earlier.[19] Hence, not only does the s-PBI membrane provide a constant ASR at all currents (i.e., sulfuric acid concentration), it also provides the potential of operating the cell at significantly elevated temperatures to reduce kinetic resistance.

## Conclusions

We have successfully operated the HyS electrolyzer using sulfuric acid-doped s-PBI membranes. Our previously reported experimental operation has been modified to permit humidification of the $SO_2$ sent to the anode instead of allowing liquid water to diffuse through the membrane. We have shown that, despite its relative thickness (almost 3 times thicker than N117, and 10 times thicker than N212), the area-specific resistance of s-PBI compares favorably with Nafion, and is not adversely affected by the sulfuric acid concentration at the anode. Also, s-PBI membranes provide the potential of operating the cell at significantly elevated temperatures to reduce kinetic resistance.

## References

1. M. B. Gorensek, *Model-based Performance Comparison of Thermochemical Nuclear Hydrogen Processes*, AIChE Spring 2005 Meeting – Session 73, presentation, April 11, 2005.
2. Department of Energy (DOE) Energy Information Administration, Hydrogen Use, Petroleum Consumption and Carbon Dioxide Emissions, Washington, DC (2008).
3. E. Varkaraki, N. Lymberopoulos, E. Zoulias, D. Guichardot, and G. Poli, *Int. J. Hydrogen Energy*, **32**, 1589 (2007).
4. Y. Shin, W. Park, J. Chang, and J. Park, *Int. J. Hydrogen Energy*, **32**, 1486 (2007).
5. J. S. Herring, J. E. O'Brien, C. M. Stoots, G. L. Hawkes, J. J. Hartvigsen, and M. Shahnam, *Int. J. Hydrogen Energy*, **32**, 440 (2007).
6. Nuclear Hydrogen R&D Plan DRAFT; Department Of Energy, Office of Nuclear Energy, Science and Technology, 2004.
7. Nuclear Hydrogen Initiative: Ten Year Program Plan, Office of Advanced Nuclear Research, DOE Office of Nuclear Energy, Science and Technology, March 2005.
8. A. Hauch, S. H. Jensen, S. Ramousse, and M. Mogensen, *J. Electrochem. Soc.*, **153**, A1741 (2006).
9. P. W. Lu, E. R. Garcia, and R. L. Ammon, *J. Appl. Electrochem.*, **11**, 347 (1981).
10. P. W. Lu and R. L. Ammon, *J. Electrochem. Soc.*, **127**, 2610 (1980).
11. P. Sivasubramanian, R. P. Ramasamy, F. J. Freire, C. E. Holland, and J. W. Weidner, *Int. J. Hydrogen Energy*, **32**, 463 (2007).
12. M. B. Gorensek and W. A. Summers, *Int. J. Hydrogen Energy*, **34**(9), 4097 (2009).
13. F. Jomard, J. P. Feraud, and J. P. Caire, *Int. J. Hydrogen Energy*, **33**, 1142 (2008).
14. J. Staser, R. P. Ramasamy, P. Sivasubramanian, and J. W. Weidner, *Electrochemical and Solid-State Letters*, **10**, E17 (2007).
15. J. A. Staser and J. W. Weidner, *J. Electrochem. Soc.*, **156**, B16 (2009).
16. J. A. Staser, K. Norman, C. H. Fujimoto, M. A. Hickner, and J. W. Weidner, *J. Electrochem. Soc.*, **156**, B842 (2009).
17. J. A. Staser and J. W. Weidner, *J. Electrochem. Soc.*, **156**, B836 (2009).
18. M. B. Gorensek, J. A. Staser, T. G. Stanford, and J. W. Weidner, *Int. J. Hydrogen Energy*, **34**, 6089 (2009).
19. J. A. Staser, M. B. Gorensek, and J. W. Weidner, *J. Electrochem. Soc.*, **157**, B952 (2010).
20. S.-K. Lee, C.-H. Kim, W.-C. Cho, K.-S. Kang, C.-S. Park, and K.-K. Bae, *Int. J. Hydrogen Energy*, **34**, 4701 (2009).
21. A. V. Anantaraman and C. L. Gardner, *J. Electroanal. Chem.*, **414**, 115 (1996).
22. M. Cappadonia, J. Wilhelm Erning, S. M. Saberi Niaki, and U. Stimming, *Solid State Ionics*, **77**, 65 (1995).
23. J. S. Wainright, J.-T. Wang, D. Weng, R. F. Savinell, and M. Litt, *J. Electrochem. Soc.*, **142**, L121 (1995).
24. J.-T. Wang, R. F. Savinell, J. Wainright, M. Litt, and H. Yu, *Electrochim. Acta*, **41**, 193 (1996).
25. L. Xiao, H. Zhang, T. Jana, E. Scanlon, R. Chen, E.-W. Choe, L. S. Ramanathan, S. Yu, and B. C. Benicewicz, *Fuel Cells*, **5**(2), 287 (2005).
26. L. Xiao, H. Zhang, E. Scanlon, L. S. Ramanathan, E.-W. Choe, D. Rogers, T. Apple, and B. C. Benicewicz, *Chem Mater.*, **17**(21), 5328 (2005).
27. J. A. Mader and B. C. Benicewicz, *Macromolecules*, **43**, 6706 (2010).
28. J. Mader and B. Benicewicz, *Fuel Cells*, **11**(2), 212 (2011).
29. A. L. Gulledge, B. Gu, and B. C. Benicewicz, *J. Pol. Sc. A: Polymer Chemistry*, **50**, 306 (2011).